Synthesis characteristics of Cu particulates in high-pressure magnetron sputtering plasmas studied by *in-situ* laser-light scattering

N. Nafarizal

Microelectronics and Nanotechnology-Shamsuddin Research Centre (MiNT-SRC), Faculty of Electrical and Electronic Engineering, University Tun Hussein Onn Malaysia, 86400 Johor, Malaysia

E-mail: nafa@uthm.edu.my

K. Sasaki

Division of Quantum Science and Engineering, Faculty of Engineering, Hokkaido University, Sapporo, Hokkaido 060-8628, Japan

E-mail: sasaki@qe.eng.hokudai.ac.jp

Abstract.

This paper reports the temporal evolution, the dependence on the discharge conditions, and the spatial distribution of Cu particulates synthesized in high-pressure magnetron sputtering plasmas. The spatial distributions of the size and the density of particulates were examined with precision using a two-wavelength laser light scattering technique. We found that more than 50% of Cu particulates in the discharge space had sizes ranging between 100 and 175 nm. The absolute density of Cu particulate was on the order of $10^7 - 10^9$ cm^{-3}. Cu particulates had concentrated distributions in the boundary between the bright plasma and the dark region and in the region connecting to the anode of the magnetron sputtering source. The spatial distribution, the size distribution, and the density of Cu particulates were sensitively dependent on the discharge power and the pressure.

PACS numbers: 81.15.Cd, 34.50.Rk, 81.07.-b

1. Introduction

Nowadays, ionized physical vapor deposition (IPVD) using a magnetron sputtering plasma has been a successful technology to deposit barrier and seed layers on the side walls and the bottoms of narrow trenches and holes for interconnections of ultralarge-scale integrated circuits (ULSIs). In our previous works, we have shown that a high-pressure condition of a magnetron sputtering plasma is useful for obtaining conformal deposition inside fine patterns [1]. We showed that the degree of ionization of metal atoms sputtered out from the target was enhanced when the gas pressure was increased to > 100 mTorr in a conventional magnetron sputtering system [2, 3].

Although the high-pressure magnetron sputtering is a promising technique for the IPVD process, the high-pressure plasma condition is also known as an efficient environment for the formation of particulates or dusty particles. The particulates are recognized as a source of contamination problems in plasma processing since it could cause circuit defects in ULSI interconnects. Therefore, attention should be paid to the growth of particulates in high-pressure magnetron sputtering plasma in order to improve the IPVD process [4–8].

Contrary to the contamination problem in microelectronics industries, particulates are of interest in numerous applications related to nanotechnology and biotechnology areas. Nanoparticles have been investigated with the intension of applying them to catalysis, photonics, and sensing technologies [9–16]. For such numerous applications, sputtering process has advantages in the repeatability and the flexibility for preparing various nanoparticles of metals and dielectric materials.

The generation and growth kinetics of particulates in plasmas have been studied using *in-situ* laser light scattering techniques by many researchers, especially in plasma-enhanced chemical vapor deposition [17, 18]. The scattering theory is based on the Lorentz-Mie scattering where the incident laser light is efficiently scattered by particles when the size of the particle is roughly the same as the laser light wavelength [19]. The advantage of this technique is that it gives a better spatial and temporal resolutions in the discharge space. In addition, the laser light scattering technique can also provide information about the mean size and the density of particulates.

In contrast to many works in plasma-enhanced chemical vapor deposition, fundamental investigation on the generation and the growth kinetics of particulates has been insufficient in physical vapor deposition. In this paper, we detected the generation of Cu particulates in the discharge space of high-pressure magnetron sputtering plasma using a laser light scattering technique. The scattered laser light was found to be concentrated at the boundary of the bright plasma and the adjacency of the anode of the magnetron source. We evaluated the mean size and the density of Cu particulates in the discharge space from the scattered laser light intensities at 457 and 672 nm.

2. Experimental setup

The magnetron sputtering system is schematically shown in Fig. 1, which is the same system as reported elsewhere [3, 8]. We used a cylindrical vacuum chamber with four large observation ports. The chamber had a diameter of 16 cm and a length of 18 cm. A conventional balanced magnetron sputtering source with a pair of cylindrical permanent magnets on an indirect water-cooling system was inserted into the vacuum chamber from the bottom. A copper (Cu) target with a diameter of 50 mm was installed on the cathode. The $z-r$ coordinate in front of the magnetron source is shown in Fig. 1. The discharge gas was argon and it was injected from the top of the pumping system as shown in Fig. 1. The gas pressure was measured using a capacitance manometer. A direct-current (dc) power supply was used for discharges.

We used two cw lasers at wavelengths of 457 and 672 nm for evaluating the size and the density of Cu particulates by a laser light scattering technique. The laser beams were arranged to have planar shapes using cylindrical lenses, and were injected into the discharge space. The planar laser beams passed through the cylindrical axis of the discharge system. The intensities of the planer laser beams were 0.3 and 0.9 mW/mm^2 at 457 and 672 nm, respectively. The scattered laser lights were detected from the normal direction to the incident laser beams using charge-coupled device cameras with image intensifiers (ICCD cameras) via interference filters at the laser wavelengths. The transmission bands of the interference filters used in the present experiment were 457 $\pm$4 nm and 670 $\pm$5 nm for laser wavelengths of 457 and 672 nm, respectively. A polarizer was placed in front of the ICCD camera to detect the scattered laser light which had the polarization perpendicular to the scattering plane. We used two types of ICCD cameras; one was for capturing still pictures of the scattered laser light and the other was for recording the temporal variation as moving pictures. The output from the ICCD camera for moving images was an analog video signal with a flame rate of 30 Hz, and was recorded on a computer using an analog-to-digital convertor with a resolution of 8 bits. A high-resolution image with a wide dynamic range was obtained using the ICCD camera for still pictures since it had a 16-bit analog-to-digital convertor. Since the raw image taken by the ICCD camera was composed of the scattered laser light, the stray light, and the self-emission of the plasma, the image of the scattered laser was obtained by subtracting the stray light and the self-emission from the raw image.

The intensity of the laser light scattered by small particles is a complex function of the size, the shape, the refractive index, and the number density of particles. It is also expressed in term of the directions, the wavelength, and the polarizations of the incident and scattered laser lights. The refractive index m is given in reference [19], which was evaluated at a particular laser wavelength by assuming spherical particulates. We evaluated the mean size of Cu particulates from the ratio of the scattered laser light intensities at 457 and 672 nm with the help of the theory of Rayleigh and Mie scattering [19–23]. The density of particulates was evaluated by the absolute scattered light intensity, which was obtained by calibrating the sensitivity of the ICCD camera

using a tungsten standard lamp with a known spectral irradiance. These measurements gave us spatial distributions of the mean size and the density of Cu particulates in the gas phase of the magnetron sputtering plasma source. Although the measurements at the two wavelengths were not carried out simultaneously, we evaluated the mean size and the density from the two measurements since we checked the reproducibility of the scattered laser lights carefully.

3. Results and discussion

3.1. Temporal evolution after the initiation of discharge

The laser light scattered by Cu particulates in high-pressure magnetron sputtering plasma was successfully detected. Figure 2 shows the temporal evolution of the image of the scattered laser light after the initiation of the discharge at a dc power of 15 W and an Ar pressure of 400 mTorr. The laser wavelength was 672 nm. We recorded a moving image in this experiment, and we picked up snap shots at various delay times after the initiation of the discharge from the moving image as shown in Fig. 2. The measurements covered a time range from 0 to 180 s after the plasma ignition.

As shown in Fig. 2(a), we observed particulates near the target at $t = 2$ s after the plasma ignition. The particulates near the target were extinguished promptly. After that, we observed particulates with a broad distribution at the boundary between the bright plasma and the dark region, as shown at in Fig. 2(b). It is noted that the bright plasma was localized in the region near the target since a conventional magnetron sputtering source was used in this experiment. The scattered laser light intensity increased with time. At $t = 40 - 60$ s, another group of the intense scattered laser light appeared in the region which was connected to the ring anode of the magnetron sputtering source. The scattered laser light intensity then changed in time slowly, and became almost stable after $t = 120$ s. Since the intensity of the scattered laser light is dependent on the mean size and the density of particulates, this result indicates that the size and/or the density of particulates shifted with the delay time after the plasma ignition.

In general, there are three main forces which contribute to the behavior of particulates in plasmas. They are the ion drag force, the electrostatic force, and the fluid force. The fluid force consists of gas flow, gravity, and thermophoresis. The observation of the stable scattered laser light intensity, which was observed at 120 s after the initiation of the discharge, suggests that a balance among the forces is realized in the steady-state plasma, and it traps particulates at the boundary between the bright plasma and the dark region and in the region which is connected to the ring anode. Since the gas temperature in the bright plasma is high, the influence of the thermophoresis may play the dominant role in trapping particulates. A similar trapping phenomena of particulates in plasmas were observed in rf capacitively coupled discharges produced between two parallel-plate electrodes [24, 25]. However, the magnetron sputtering

plasma has more complex magnetic and electric field structures than the parallel-plate rf discharges do, so that further investigations on the generation kinetics of particulates in magnetron sputtering plasmas are necessary.

3.2. Influence of discharge conditions

Figure 3 shows the distributions of the scattered laser light intensity observed at various dc powers. The pictures shown in Fig. 3 were picked up from moving images at approximately 120 s after the initiation of the discharges. The laser wavelength was 672 nm, and the Ar pressure was fixed at 400 mTorr. At a dc power of 5 W, as shown in Fig. 3(a), we observed a broad distribution of the scattered laser light intensity in the region outside the bright plasma. At a dc power of 15 W, as described in the previous section, the region with particulates was separated into two groups (Fig. 3(b)).

The scattered laser light intensity decreased drastically when the dc power was increased to 25 W. The peak of the scattered laser light intensity was observed at the outer edge of the observation area, as shown in Fig. 3(c). On the other hand, no scattered laser light was detected even in a low dc power when the gas pressure was lower than 200 mTorr. The scattered laser light intensity below the detection limit is due to a small amount or a small size of particulates. The sensitive dependence of the production efficiency of particulates on the discharge conditions is useful information for both producing and avoiding nanoparticles in plasmas.

3.3. Evaluations of size and density of particulates

We carried out the scattering measurements at the two laser wavelengths of 457 and 672 nm, to evaluate the mean size and the density of Cu particulates. Figure 4 shows the distributions of the scattered laser light intensities and their ratios. The dc power and the Ar pressure were 4 W and 400 mTorr, respectively. These results were obtained in a steady-state plasma at a sufficiently long delay time after the initiation of the discharge. The ICCD camera for a still picture was used in this measurement. The vertical axes of Figs. 4(a) and 4(b) are proportional to the photon number. They can be compared each other since the vertical axes are normalized by the intensities of the incident laser beams.

As shown in Figs. 4(a) and 4(b), the spatial distributions of the scattered laser light intensities at the two laser wavelengths were roughly similar. The peak position of the scattered laser light intensities were located adjacent to the ring anode of the magnetron sputtering source. However, it is found with close attention to details in Fig. 5 that the scattered laser light intensity was dependent on the laser wavelength. As shown in Fig. 4(c), the ratio of the scattered laser light intensities at 457 and 672 nm was high at the boundary between the bright plasma and the dark region. On the other hand, the intensity ratios in the region near the anode ring and in the region at a long distance from the bright plasma were low.

We calculated the ratio of the scattered laser light intensities at 457 and 672 nm as a function of the size of particulates using a conventional theory [19] as shown in Fig. 5. It is known from Fig. 5 that the ratio of the scattered laser light intensities is almost independent of the size of particulates if the diameter of particulates is smaller than 80 nm. In addition, there is an overlapping in the ratio of the scattered laser light intensities when the diameter of particulates is larger than 320 nm. Because of these limitations, we evaluated the size of particulates in the diameter range between 80 and 320 nm.

The distributions of the size and the density of Cu particulates are shown in Fig. 6. Figures 6(a) and 6(c) clearly indicate that particulates with larger sizes were observed in the neighboring region to the ring anode of the magnetron source, while particulates with smaller sizes were observed in the boundary between the bright plasma and the dark region. On the other hand, as shown in Figs. 6(b) and 6(d), Cu particulates had the peak density in the boundary between the bright plasma and the dark region. The density of Cu particulates decreased drastically with the distance from the bright plasma region. The absolute density of Cu particulates ranged from 10^7 to 10^9 cm^{-3}.

The histogram of the diameter of Cu particulates, which was obtained by counting the appearance frequency of the diameter in the two–dimensional distribution of Figs. 6(a) and 6(b), is shown in Fig. 7. The discharge pressure was 400 mTorr, and the rf powers were 4 and 7 W in Figs. 7(a) and 7(b), respectively. It was observed that the frequency of particulates with diameters less than 100 nm decreased drastically when the dc power was increased from 4 to 7 W. As shown in Fig. 7(b), at a dc power of 7 W, more than 50% of particulates had diameters ranging between 100 and 175 nm. The abundance of particulates with diameters smaller than 100 nm was less than 2%. On the other hand, at a dc power of 4 W, the abundance of particulates with diameter smaller than 100 nm was more than 10% as shown in Fig. 7(a). In recent researches, it has been reported that the properties of thin films with embedded nanoparticles are closely related to the size of embedded particulates [13–15]. The result shown in Fig. 7 is a useful information on the relationship between the size of particulates and the discharge power in the synthesis of nanoparticles by magnetron sputtering. Furthermore, there have been intensive works showing that the growth of nano-clusters ranging between 1 and 100 nm is sensitive to the sputtering power, the gas pressure, the gas flow rate, and the aggregation distance [26–31].

3.4. SEM observation

In order to verify the size of particulates examined by *in-situ* laser light scattering, we collected Cu particulates on a stainless-steel substrate and observed them using a scanning electron microscope (SEM). We applied a bias voltage of +20 V with respect to the ground potential to the substrate to collect particulates efficiently. The discharge power and gas pressure were 4 W and 400 mTorr, respectively, and the deposition time was 30 minutes. Figure 8 shows an SEM image of Cu particulates collected on a stainless-

steel substrate. As shown in Fig. 8, the shape of particulates was roughly spherical, and their diameters were approximately 100 nm, which was a consistent size with the one evaluated by laser light scattering. The comparison with the SEM observation indicates the validity of the size of particulates evaluated by laser light scattering.

4. Summary

In this work, we examined the temporal evolution and the spatial distribution of Cu particulates produced in high-pressure magnetron sputtering plasmas using a laser light scattering technique. In addition, we reported the spatial distributions of the density and the size of Cu particulates observed in steady-state plasmas. We found that Cu particulates were concentrated at the boundary between the bright plasma and the dark region and in the region connecting to the ring anode of the magnetron sputtering source. The distribution, the density, and the size of particulates were sensitively dependent on the discharge conditions. The experimental results shown in this paper are useful for both synthesizing and avoiding particulates in magnetron sputtering plasmas.

Acknowledgments

The authors would like to express their gratitude to Dr. N. Takada of Nagoya University for his support in this work.

[1] Nafarizal N, Takada N, Nakamura K, Sago Y, and Sasaki K 2006 *J. Vac. Sci. Technol. A* **24** 2206
[2] Nafarizal N, Takada N, Shibagaki K, Nakamura K, Sago Y and Sasaki K 2005 *Jpn. J. Appl. Phys.* **44** L737
[3] Nafarizal N, Takada N and Sasaki K 2009 *Jpn. J. Appl. Phys.* **48** 126003
[4] Shiba K, Wakabayashi H, Takewaki T, Kikuta K, Kubo A, Yamasaki S and Hatashi Y 1999 *Jpn. J. Appl. Phys.* **38** 2360
[5] Rossnagel S M and Hopwood J 1993 *Appl. Phys. Lett.* **63** 3285
[6] Rossnagel S M and Hopwood J 1994 *J. Vac. Sci. Technol. B* **12** 449
[7] Lu J and Kushner M J 2001 *J. Vac. Sci. Technol. A* **19** 2652
[8] Sasaki K and Nafarizal N 2010 *J. Phys. D* **43** 124012
[9] L Armelao, D Barreca, G Bottaro, A Gasparotto, S Gross, C Maragno and E Tondello 2006 *Coordinat. Chem. Rev.* **250** 1294.
[10] C C Berry and A S G Curtis 2003 *J. Phys. D* **36** R198
[11] A K Gupta and M Gupta 2005 *Biomaterials* **26** 3995
[12] H Kersten, H Deutsch, E Stoffels, W W Stoffels and G M W Kroesen 2003 *Int. J. Mass Spectroscopy* **223-224** 313
[13] Y Lei, W Cai and G Wilde 2007 *Prog. Mater. Sci.* **52** 465
[14] L Dreesen, J F Colomer, H Limage, A Giguere and S Lucas 2009 *Thin Solid Films* **518** 112
[15] M Yoshinaga, K Yamamoto, N Sato, K Aoki, T Morikawa and A Muramatsu 2009 *Applied Catalysis B: Enviromental* **87** 239
[16] K Wegner, P Piseri, H V Tafreshi and P Milani 2006 *J. Phys. D* **39** R439
[17] Watanabe Y 2006 *J. Phys. D: Appl. Phys.* **39** R329
[18] Bouchoule A ed. 1999 *Dusty Plasmas* (John Wiley & Sons, Chichester)
[19] H C van de Hulst: *Light Scattering by Small Particles* (Dover, New York, 1981).

[20] Ch Hollenstein, J L Dorier, J Dutta L Sansonnens and A A Howling 1994 *Plasma Sources Sci. Technol.* **3** 278
[21] C Courteille, Ch Hollenstein, J L Dorier, W Schwarzenbach, E Bertran, G Viera, R Martins and A Macarico 1996 *J. Appl. Phys.* **80** 2069
[22] A Plain 1998 *J. Appl. Phys.* **83** 4012
[23] S Nunomura, M Kita, K Koga, M Shiratani and Y Watanabe 2006 *J. Appl. Phys.* **99** 083302
[24] S M Collins, D A Brown, J F O'Hanlon and R N Carlile 1996 *J. Vac. Sci. Technol. A* **14** 634
[25] D Samsonov and J Goree 1999 *J. Vac. Sci. Technol. A* **17** 2835
[26] H Haberland, M Mosseler, Y Qiang, O Rattude, T Reiners and Y Thuner 1996 *Surf. Rev. Lett.* **3** 887
[27] S R Bhattacharyya, D Datta, I Shyjumon, B M Smirnov, T K Chini, D. Ghose and R Hippler 2009 *J. Phys. D: Appl. Phys.* **42** 035306
[28] S Protontep, S J Carroll, C Xirouchaki, M Streun and R E Palmer 2005 *Rev. Sci. Instrum.* **76** 045103
[29] I Shyjumon, M Gopinadhan, C A Helm, B M Smirnov and R Hippler 2006 *Thin Solid Films* **500** 41
[30] B M Smirnov, I Shyjumon and R Hippler 2006 *Phys. Scr.* **73** 288
[31] P V Kashtanov, B M Smirnov and R Hippler 2007 *Physics Uspekhi* **50** (5) 455

Figure captions

Fig.1 Experimental apparatus for applying a laser light scattering technique to a magnetron sputtering plasma source.

Fig.2 Temporal evolution of Cu particulates after igniting a plasma at a dc power of 15 W and an Ar pressure of 400 mTorr.

Fig.3 Spatial distributions of the scattered laser light intensities observed at various dc power. The Ar pressure was fixed at 400 mTorr.

Fig.4 Spatial distributions of the scattered laser light intensities at (a) 672 and (b) 457 nm. The ratio of the scattered laser light intensities at the two wavelengths is shown in (c). The dc power and the Ar pressure were 4 W and 400 mTorr, respectively.

Fig.5 Result of theoretical calculation on the ratio of the scattered laser light intensities at 457 and 672 nm as a function of the diameter of Cu particulates.

Fig.6 Spatial distributions of the diameter and the density of Cu particulates evaluated by two-wavelength laser light scattering. (a) and (b) are the diameter and the density observed at a dc power of 4 W, while (c) and (d) are the diameter and the density observed at a dc power of 7 W. The Ar pressure was fixed at 400 mTorr.

Fig.7 Size distribution of Cu particulates observed at dc powers of (a) 4 W and (b) 7 W. The Ar pressure was fixed at 400 mTorr.

Fig.8 SEM image of Cu particulates collected on a stainless-steel substrate. The dc power and the Ar pressure were 4 W and 400 mTorr, respectively.

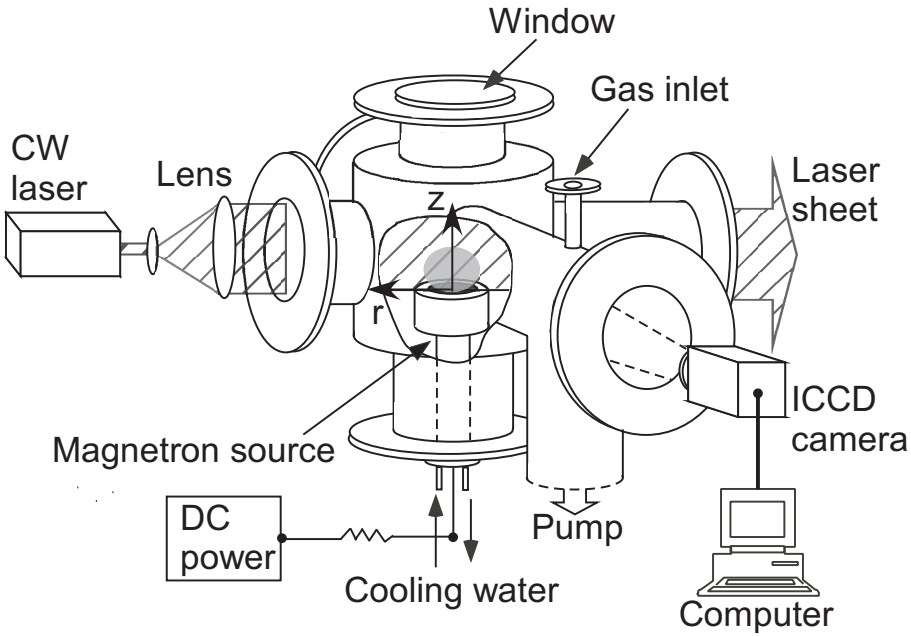

Figure 1. Experimental apparatus for applying a laser light scattering technique to a magnetron sputtering plasma source.

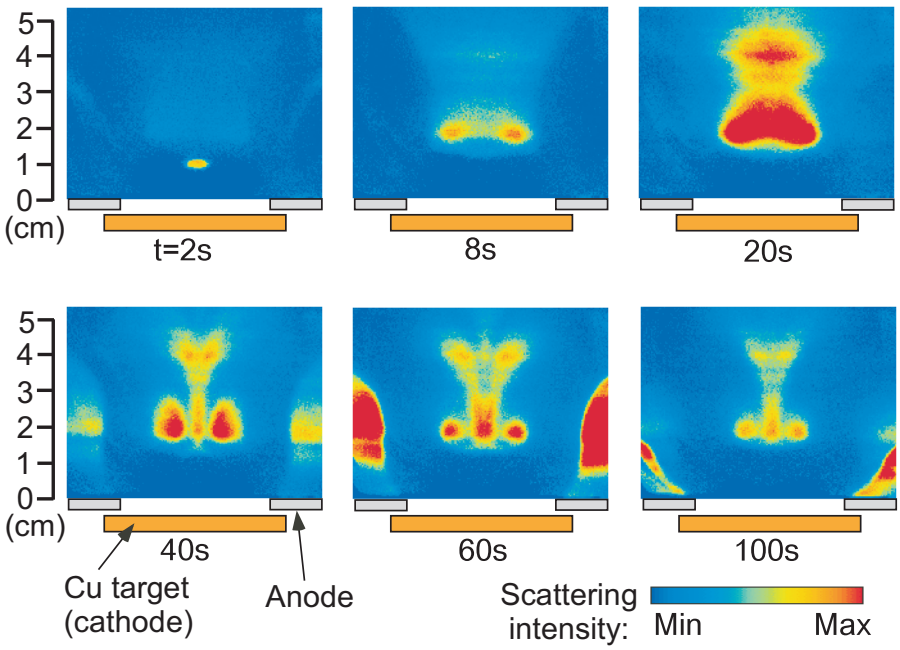

Figure 2. Temporal evolution of Cu particulates after igniting a plasma at a dc power of 15 W and an Ar pressure of 400 mTorr.

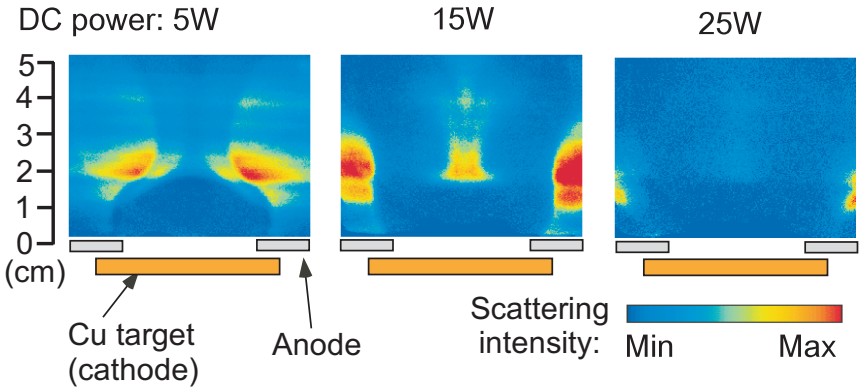

Figure 3. Spatial distributions of the scattered laser light intensities observed at various dc power. The Ar pressure was fixed at 400 mTorr.

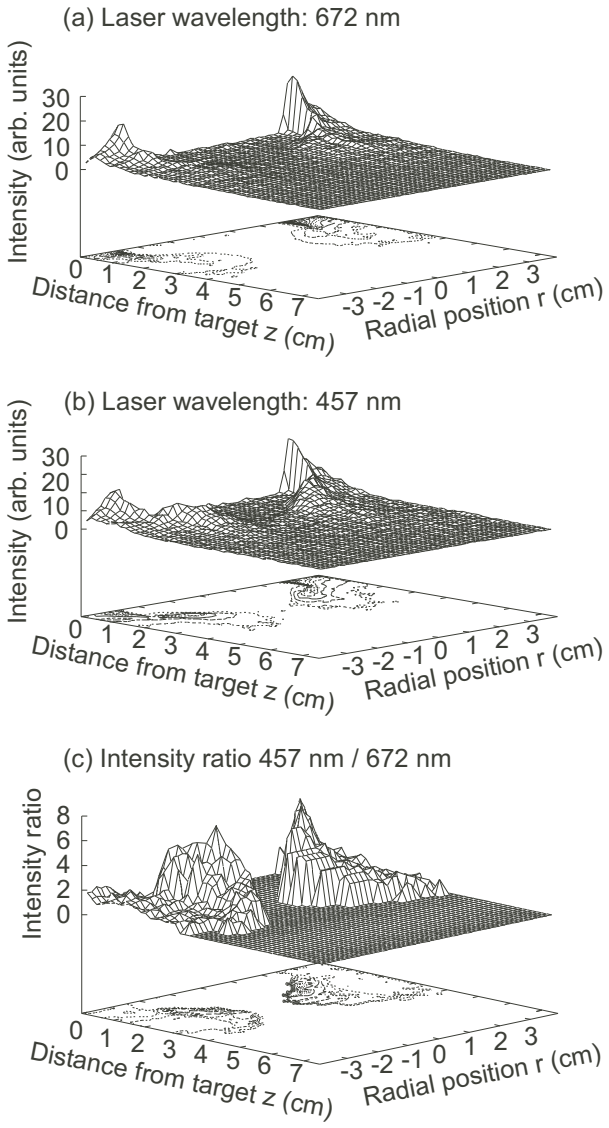

Figure 4. Spatial distributions of the scattered laser light intensities at (a) 672 and (b) 457 nm. The ratio of the scattered laser light intensities at the two wavelengths is shown in (c). The dc power and the Ar pressure were 4 W and 400 mTorr, respectively.

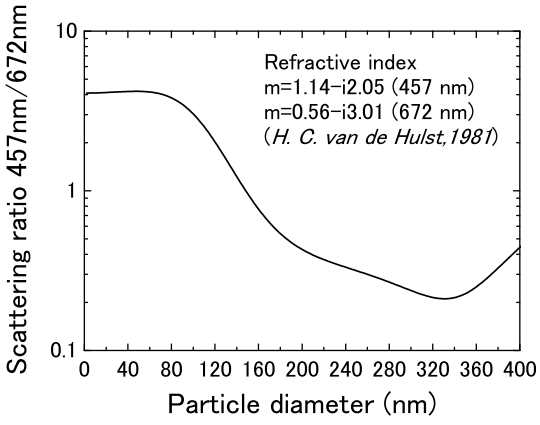

Figure 5. Result of theoretical calculation on the ratio of the scattered laser light intensities at 457 and 672 nm as a function of the diameter of Cu particulates.

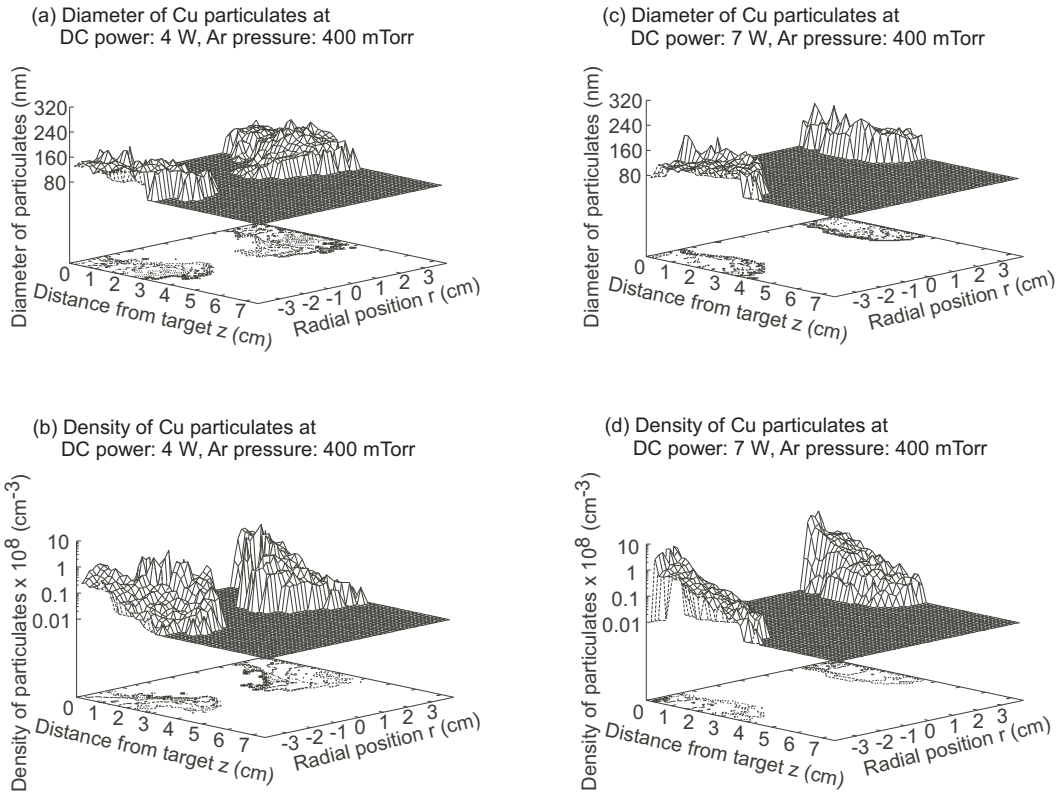

Figure 6. Spatial distributions of the diameter and the density of Cu particulates evaluated by two-wavelength laser light scattering. (a) and (b) are the diameter and the density observed at a dc power of 4 W, while (c) and (d) are the diameter and the density observed at a dc power of 7 W. The Ar pressure was fixed at 400 mTorr.

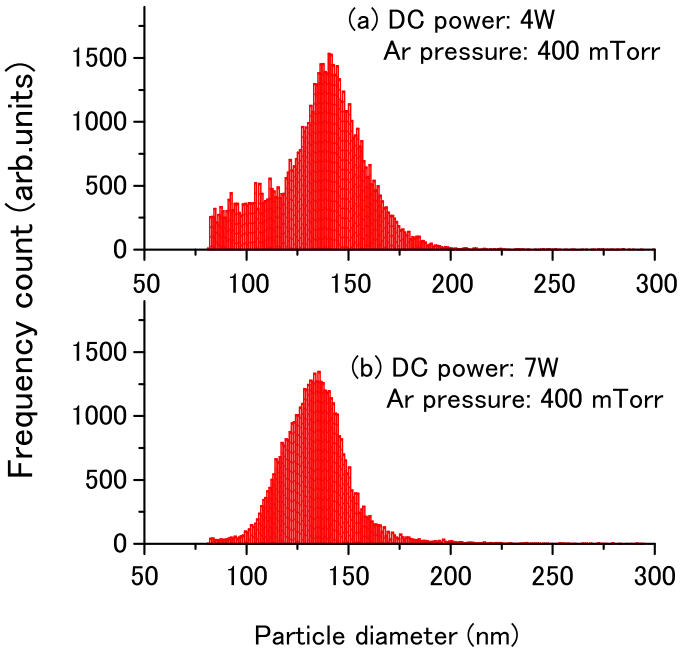

Figure 7. Size distribution of Cu particulates observed at dc powers of (a) 4 W and (b) 7 W. The Ar pressure was fixed at 400 mTorr.

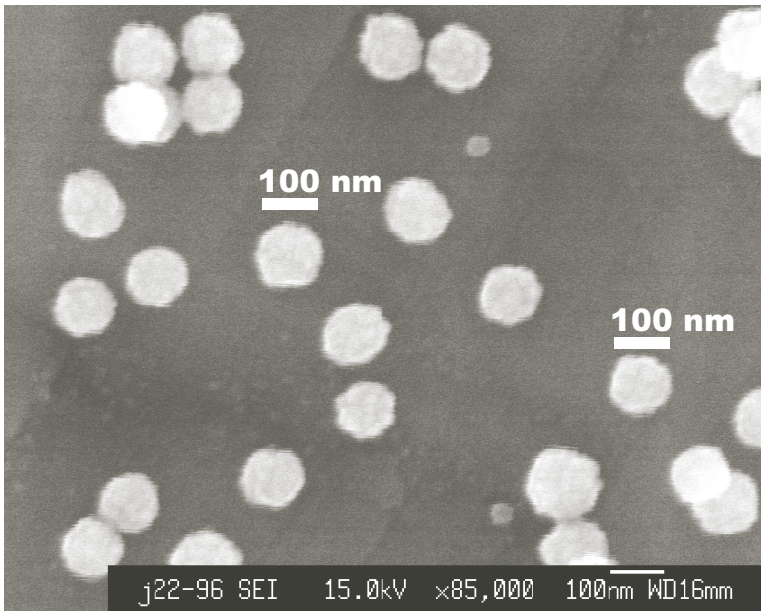

Figure 8. SEM image of Cu particulates collected on a stainless-steel substrate. The dc power and the Ar pressure were 4 W and 400 mTorr, respectively.